Santiago Bogarra, Antoni Garcia, Manuel Moreno-Eguilaz, Jordi-Roger Riba. (2018) Detailed off-line parameter identification of synchronous generator based on frequency response tests. Proceedings: 2018 IEEE 18th International Conference on Power Electronics and Motion Control (PEMC): The Budapest Congress and World Trade Center Budapest, Hungary 26 - 30 August, 2018 . Pp. 906-911
Doi: http://dx.doi.org/10.1109/EPEPEMC.2018.8521865.

Santiago Bogarra, Antoni Garcia, Manuel Moreno-Eguilaz, Jordi-Roger Riba. (2018) Detailed off-line parameter identification of synchronous generator based on frequency response tests. Proceedings: 2018 IEEE 18th International Conference on Power Electronics and Motion Control (PEMC): The Budapest Congress and World Trade Center Budapest, Hungary 26 - 30 August, 2018 . Pp. 906-911
Doi: http://dx.doi.org/10.1109/EPEPEMC.2018.8521865.

Detailed off-line parameter identification of Synchronous generator based on frequency response tests

Santiago Bogarra[1], Antoni Garcia[1], Manuel Moreno-Eguilaz[1], Jordi-Roger Riba[1]
[1] Universitat Politècnica de Catalunya, Rambla Sant Nebridi 22, 08222 Terrassa (Barcelona, Spain)
Topic number: Educational

***Abstract*— This work presents a general methodology, based on standstill frequency response tests. Once the circuit topology is chosen, it allows a systematic calculation of the circuit parameters for a salient pole synchronous generator. The order of the circuit considered can be whatever, even a customized circuit topology, since the methodology does not rely on a specific formulation. The transfer function coefficients are expressed as a function of the circuit parameters by using the symbolic Matlab toolbox. From tests, the coefficients of the transfer function are fitted in both axes. Then the coefficients have to match with the symbolic transfer function previously obtained in order to calculate the circuit parameters. If the dynamic behavior obtained with the fitted parameters is not accurate enough, the circuit order is increased until attaining an accurate solution. This methodology results in a useful educational tool for machine characterization. Nowadays many methods are found in the technical literature to calculate such parameters, although most of them computationally demanding.**

***Index Terms*— Synchronous generator, standstill tests, equivalent circuit, identification parameters.**

NOMENCLATURE

e_d	*d*-axis armature voltage [V]
e_q	*q*-axis armature voltage [V]
e_{fd}	Field voltage [V]
v_{arm}	voltage between two armature terminals during test [V]
i_d	*d*-axis armature current [A]
i_q	*q*-axis armature current [A]
i_{fd}	Field current [A]
i_{arm}	Armature current during test [A]
R_a	Armature resistance [Ω]
R_{fd}	Field resistance referred to the armature [Ω]
R_{kd}	*d*-axis damper winding resistance, *k =1,2…n* [Ω]
R_{kq}	*q*-axis damper winding resistance, *k =1,2…n* [Ω]
L_l	Armature leakage inductance [H]
L_{ad}	*d*-axis armature to rotor mutual inductance [H]
L_{aq}	*q*-axis armature to rotor mutual inductance [H]
L_{fd}	Field winding leakage inductance [H]
L_{kd}	*d*-axis damper winding leakage inductance, *k =1,2…n* [H]
L_{kq}	*q*-axis damper winding leakage inductance, *k =1,2…n* [H]
$L_d(s)$	*d*-axis operational inductance
$L_q(s)$	*q*-axis operational inductance
T'_{d0}	*d*-axis open circuit transient time constant [s]
T''_{d0}	*d*-axis open circuit subtransient time constant [s]
T'_{q0}	*q*-axis open circuit transient time constant [s]
T''_{q0}	*q*-axis open circuit subtransient time constant [s]
T'_d	*d*-axis short circuit transient time constant [s]
T''_d	*d*-axis short circuit subtransient time constant [s]
T'_q	*q*-axis short circuit transient time constant [s]
T''_q	*q*-axis short circuit subtransient time constant [s]
$Z_{armd}(s)$	operational impedance measured between two armature terminals during *d*-axis tests
$Z_{armq}(s)$	operational impedance measured between two armature terminals during *q*-axis tests
$Z_d(s)$	*d*-axis operational impedance
$Z_q(s)$	*q*-axis operational impedance
$G(s)$	Armature to field transfer function
$Z_{afo}(s)$	Armature to field transfer impedance
SSFR	Standstill Frequency Response

I. INTRODUCTION

NOWADAYS there is a trend to move towards the "more electric aircraft", that is, replace hydraulic and pneumatic sources of power to relay on electrical power, such as actuators, deicing, engine-start or cabin air-conditioning among others. As a consequence, the electrical power requirement is expected to easily overpass 1 MW. Typical aircraft generators are rated 120 kVA, so new electrical system architectures are expected [1], although the core of the system is still the synchronous generator. On the other hand, regarding the machine's modelling, the Park's model has survived until now. By adding resistor-inductance branches, more effects can be modelled, such as second or third order effects. In the literature, the second order model for synchronous machine is referred SSFR2, whereas the third order is known as SSFR3. By means of these models, different effects can be studied, for example calculation of voltage regulation, fault identification and analysis, small and large disturbance analysis, exciters designs or high performance controllers development [2]. In this context the need of a reliable and feasible set of circuit parameters is mandatory, this still being a challenging research topic.

Parameter identification is classified into two methods, i.e. off-line and on-line identification respectively. In off-line methods the machine is out of service. Among them, one can find open circuit frequency response, dc-excitation methods and standstill frequency response [3], which is used in the IEEE Std. 115-A, and in the methodology of this work.

However, the determination of the subtransient reactances in both axes, under saturation conditions is crucial for the calculation of the electrical and mechanical integrity of the machine during a three phase or two phase short-circuit [4].

978-1-5386-4198-9/18/$31.00 ©2018 IEEE

Besides, the estimation of the machine flux linkages is difficult, due to the strong saturation in the operation of the machine, which in turn causes the cross-saturation effect.

Thus, flux-linkages are function of both *d* and *q* axis currents, although the standstill frequency response modelling is used here because the *d* and *q* axis are decoupled. Moreover, this method allows an accurate determination of high order models since the sinusoidal signal can excite almost all frequencies with the same amplitude. Besides, the sinusoidal signals are easy to noise decorrelation [5]. This parameter estimation methodology consists on extracting the time constants applying curve-fitting and then the equivalent circuit parameters are obtained by solving a set of non-linear equations. In the literature these non-linear equations are solved through numerical optimization, although this is a process full of numerical difficulties [6-8].

It should be noted that on-line methods are receiving much attention because of their minimal impact and interference on the operation of the machine, which is in service [9-12], such that no interference occurs in the operation of the system. Mainly they belong to time domain tests, since they apply a small perturbation on the machine terminals, standstill time domain test, and load rejection test, but the standstill frequency response test is still used because its reliability its harmlessness to the machine with a relatively simple measurement set-up.

Furthermore, on-line identification methods can be classified into three categories, white-box, black-box and grey-box modelling. The white box modelling, knows exactly the topology of the system the parameters to be calculated or estimated, that is exists a theoretical model because the physical knowledge is known a priori. Among them, the extended Kalman filter [13], conjugate gradient method, neural networks, maximum likelihood, evolutionary programming, orthogonal series functions, and Hartley series can be found in the literature [14]. The black box however, is based on the input-output data because no physical knowledge is known, in such a way that is known as a data driven model. On the other hand the grey box is in between, is a hybrid model wherein the analytical equations and input-output data relations are used to obtain the parameters of the model. In this context a white model is used here because the topology of the circuit is known and the order is assumed.

Taking into account an educational approach, it is very important to present to the students a tool able to calculate the parameters involved in the dynamic equivalent circuit, i.e *d-q* axis. In this context, a new tool has been developed in Matlab®. Firstly the order of the circuit is chosen by the user, then it results in different transfer functions. These transfer function parameters are fitted with the set of experimental tests, such tests are those stated in IEEE Std. 115-A. The user can increase the circuit order if the results are not accurate enough.

The work is divided into five sections. In Section II is presented the required tests, based on the IEEE Std. 115-A, on *d-q* axis for data extraction. Section III develops the general methodology for machine parameters determination. Section IV presents the obtained results and its validation. Finally, Section V presents the conclusions.

II. Standstill Frequency Response Tests

In this work a method based on IEEE Std 115A-1987 is described for obtaining synchronous machine parameters by performing frequency response tests with the machine at standstill. Usually the second order *d*- and *q*-axis equivalent circuits, Fig. 1 and Fig. 2, are used to analyze the synchronous machine stability.

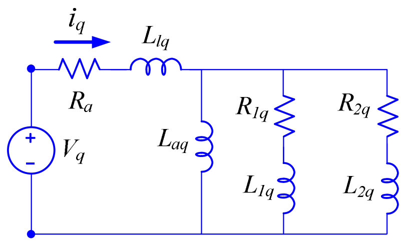

Fig.1. *q*-axis equivalent circuit

The procedure for calculating the synchronous machine parameters requires curve-fitting techniques, which are applied in an easy and intuitive way by using the Matlab software.

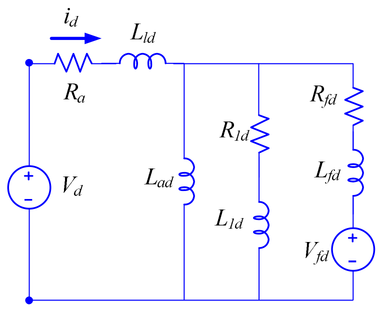

Fig.2. *d*-axis equivalent circuits

The *d*- and *q*-axis operational impedances are respectively

$$Z_d(s) = R_a + s \cdot L_d(s) \tag{1}$$

$$Z_q(s) = R_a + s \cdot L_q(s) \tag{2}$$

and both can be evaluted through small changes in the armature voltage and current when the field winding is short-circuited, by positioning the rotor, respectively, for *d*- and *q*-axis tests:

$$Z_d(s) = -\left.\frac{\Delta e_d(s)}{\Delta i_d(s)}\right|_{\Delta e_{fd}=0} \tag{3}$$

$$Z_q(s) = -\left.\frac{\Delta e_q(s)}{\Delta i_q(s)}\right|_{\Delta e_{fd}=0} \tag{4}$$

Additional measures must be taken into account depending on the order *d*- and *q*-axis equivalent circuits required to simulate accurately the transient behaviour of the synchronous machine. These measurable parameters are the armature to field transfer function, $G(s)$, and the armature to field transfer impedance, $Z_{afo}(s)$. The armature to field transfer function can be evaluted through small changes in the field and armature currents when the field winding is short-circuited:

$$sG(s) = \left.\frac{\Delta i_{fd}(s)}{\Delta i_d(s)}\right|_{\Delta e_{fd}=0} \tag{5}$$

While the armature to field transfer impedance can be evaluated through small changes in field voltage and armature current when the field winding is in open-circuit:

$$Z_{afo}(s) = -\frac{\Delta e_{fd}(s)}{\Delta i_d(s)}\bigg|_{\Delta i_{fd}=0} \quad (6)$$

In order to show how the general methodology based on standstill frequency response works, the second order *d*- and *q*-axis equivalent circuits are chosen, but this methodology can be applied to other equivalent circuits that can be found in IEEE Std 115-A. If second order equivalent circuits are chosen, then only two measurable parameters are required over a range of frequencies, the *d*- and *q*-axis operational impedances.

The first step is to position the rotor for *d*-axis tests by doing the connections shown in Fig. 3. After that, the amplifer is set to approximately 100 Hz. The next step is to turn the rotor slowly until the observed field voltage is null. When this condition is accomplished, the magnetic axis of the field winding is aligned with the series connection of phase *a* and *b*.

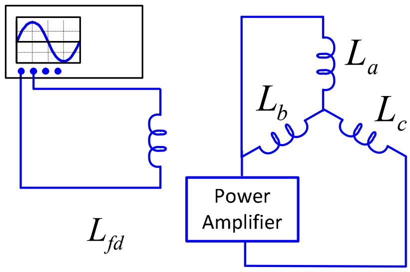

Fig. 3. Positioning the rotor for d-axis tests

After the *d*-axis is positioned the *d*-axis tests can be started by doing the connections shown in Fig. 4., where armature phases *a* and *b* are supplied by using a variable frequency power amplfier, and phase *c* is in open-circuit.

The field circuit will be short circuited with a non-inductive metering shunt. Connect the voltage and current measurements of the stator winding to the measurement instrument. Perform the measurement over a bandwidth from 0,001Hz to 1000Hz.

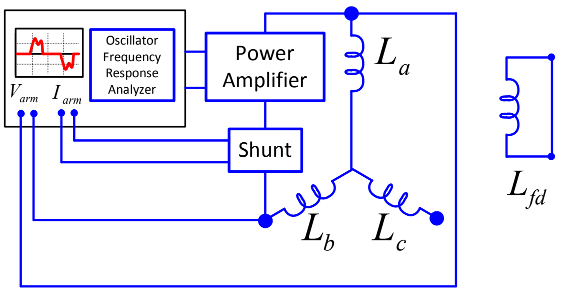

Fig. 4. d- axis impedance transfer function test

Similarly, once the *q*-axis is positioned the *q*-axis tests can be started by doing the connections shown in Fig. 5. The field circuit will be short circuited as aforementioned and the same bandwidth is applied, as presented in Fig.6.

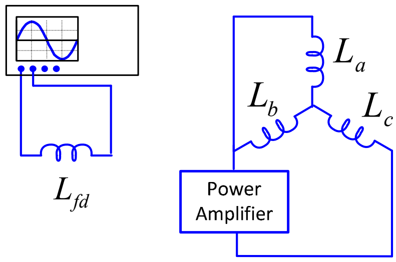

Fig. 5. Wiring of armature and field winding for rotor positioning for quadrature axis test

III. Methodology

The design methodology proposed in this work starts with the definition of the topology of *d-q* axis circuits. As already explained, in this work a SSFR2 is used, although it must be noted that this methodology can be properly applied to whatever circuit representation.

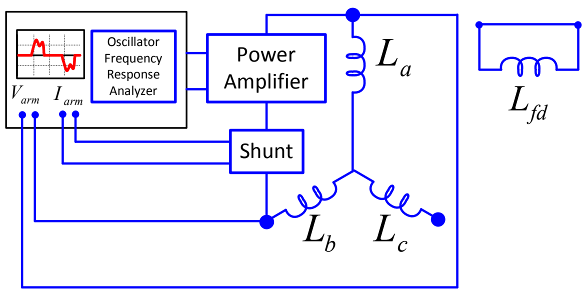

Fig. 6. Quadrature axis impedance transfer function test

The leakage inductance is needed, so it can be obtained from the zero power factor test or from the manufacturer.

A. *d-axis parameters from tests*

From the *d*-axis impedance transfer function test, the armature voltage and current are measured depending on the frequency, so the operational impedance measured between two armature terminals during the *d*-axis tests, Z_{armd}(s), can be calculated from its relation. Due to the series connection of the windings in this test, the d-axis operational impedance is calculated as:

$$Z_d = \frac{Z_{arm}}{2} \quad (7)$$

The result is shown in Fig. 7

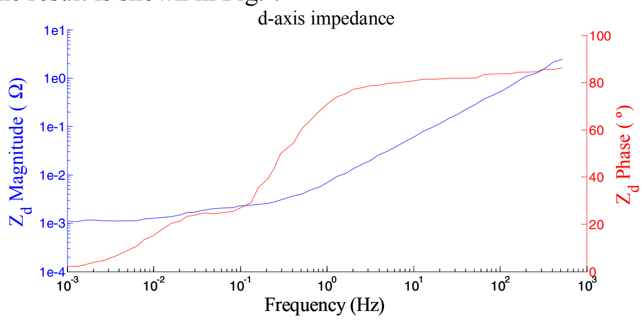

Fig. 7. *d*-axis impedance

The armature resistance, R_a, can be obtained from the real component of $Z_d(s)$ extrapolated at zero frequency.
The operational inductance in the *d*-axis is,

$$L_d(s) = \frac{Z_d(s) - R_a}{s} \quad (8)$$

The d-axis inductance at zero frequency $L_d(0)$ can be calculated extrapolating $L_d(s)$ to zero frequency as shown Fig. 8.

The direct-axis armature to rotor mutual inductance is obtained from the difference between the *d*-axis inductance at zero frequency and the leakage inductance as follows:

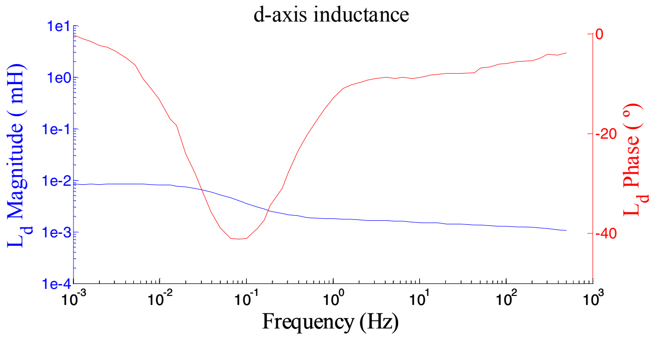

Fig. 8. *d*-axis inductance

$$L_{ad} = L_d(0) - L_l \quad (9)$$

B. d-axis equations set

The first step is to define the symbolic parameters that are represented in the equivalent circuit. The following steps consist on the association of the components in order to obtain the symbolic transfer function. The time constants presented in equation (#), which depends on the circuit order, are fitted with the experimental data shown in Fig. 8.

$$L_d(s) = \frac{L_d(0)\cdot(1+s\cdot T'_d)\cdot(1+s\cdot T''_d)}{(1+s\cdot T'_{d0})\cdot(1+s\cdot T''_{d0})} \quad (10)$$

$L_d(0)$ is the direct axis inductance in the low frequency bandwidth.

The fitted coefficients are equal to the corresponding constant time in the transfer function. In this way, an equation system can be obtained in order to find the parameters of the circuit. It must be solved in order to obtain the rest of the model parameters in Fig. 2, that is, L_{fd}, L_{1d}, R_{1d}, L_{fd} .

C. q-axis parameters

As, in d-axis, the armature impedance measurement for each sampling frequency will be obtained from the quadrature axis impedance transfer function test, from which the quadrature-axis operational impedance is obtained, as shown in equation

$$Z_q = \frac{Z_{arm}}{2} \quad (11)$$

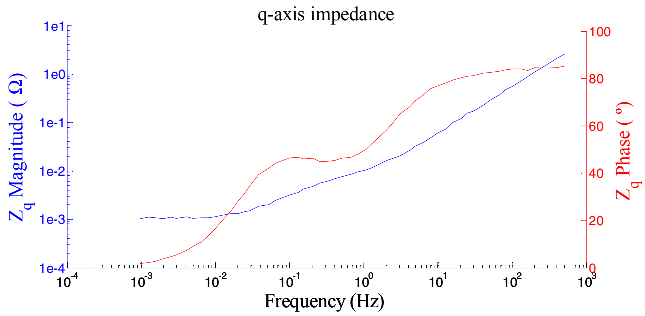

Fig. 9. *q*-axis impedance

The quadrature operational inductance is

$$L_q(s) = \frac{Z_q(s) - R_a}{s} \quad (12)$$

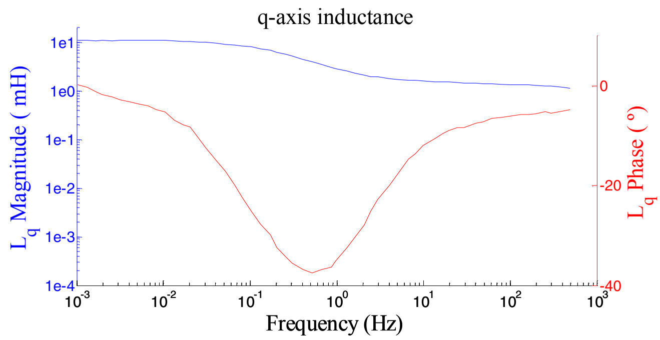

Fig. 10. *q*-axis inductance

The q-axis inductance at zero frequency $L_q(0)$ can be calculated extrapolating $L_q(s)$ to zero frequency. And similar to equation (9), from this value subtracting the leakage inductance the quadrature inductance is calculated

$$L_{aq} = L_q(0) - L_l \quad (13)$$

D. q-axis equations set

By means of the same procedure the rest of the model parameters for q-axis equivalent circuit L_{1q}, R_{1q}, L_{2q}, R_{2q}, are determined by curve-fitting technique from the operational $L_q(s)$.

$$L_q(s) = \frac{L_q(0)\cdot(1+s\cdot T'_q)\cdot(1+s\cdot T''_q)}{(1+s\cdot T'_{q0})\cdot(1+s\cdot T''_{q0})} \quad (14)$$

$L_q(0)$ is the direct axis inductance in the low frequency bandwidth.

The algorithm applied on both axes, for this purpose is exposed below.

1: Set the d-q circuits SSFR**i** order, or another customized circuit topology.
2: Obtain module and argument of d-axis operation impedance
3: Obtain resistance of armature
4: Obtain module and argument of d-axis operation inductance

6: Determination time constants

Curve fitting: **invfreqs** command from Matlab care must be taken when choosing the weighting factors.

5: Obtain set of equations by means of symbolic toolbox

children and **collect** Matlab commands to properly equation manipulation

6: Solve set of equations, **fsolve** command from Matlab

7: **If** with the obtained parameters, the dynamic simulated behavior of the machine does not agree with experimental data **then** go to 1 else

8: end

For the sake of better understanding the scheme of the procedure is shown in Fig. 11.

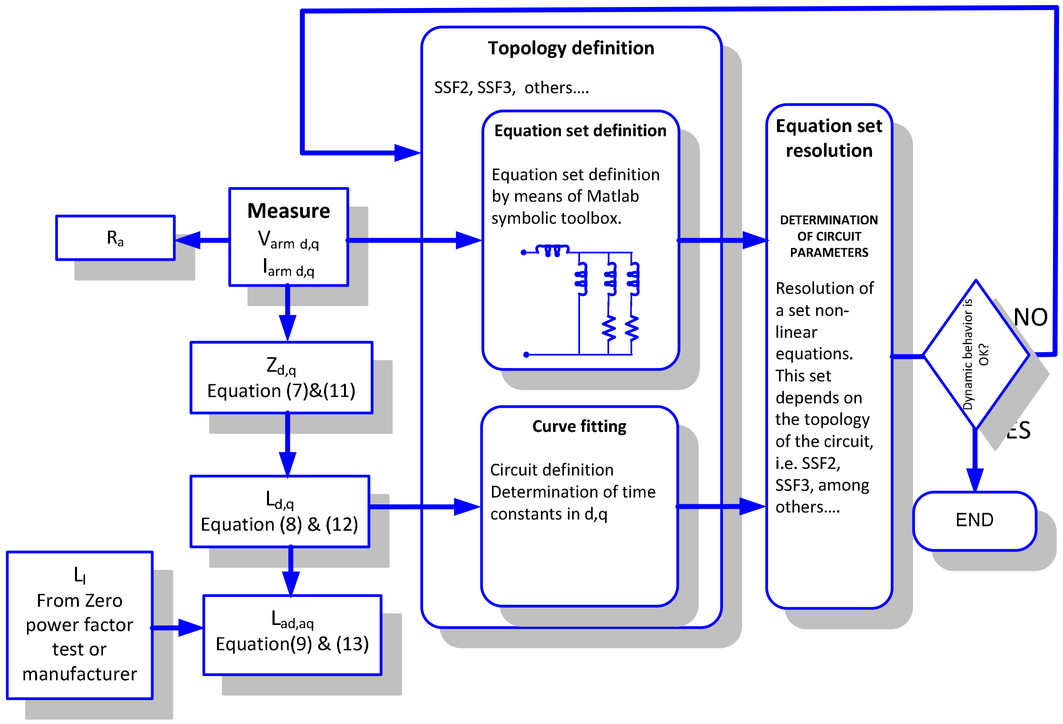

Fig. 1. Algorithm flow chart

To summarize, the procedure is based on, firstly the order of the circuit is chosen by the user, topology definition, then it results in different transfer functions, i.e equation set definition, by means of the symbolic toolbox of Matlab®. These transfer function parameters are fitted with the set of experimental tests using the aforesaid commands.

These tests are stated in IEEE Std. 115-A. This results in a iterative procedure where the user can increase the circuit order if the results are not accurate enough.

The armature resistance as well as the leakage inductance are previously obtained from DC test and zero power factor test.

IV. RESULTS AND VALIDATION

The proposed methodology approach is applied to that machine used in the Std. as an example, in order to validate the obtained results, for the sake of clarity here indicated, i.e. 192.8 MVA, 18 kV, 60 Hz.

The obtained results are shown in Fig. 12 and Fig. 13, where are plotted the measured frequency response of the machine and the frequency response calculated using the parameters extracted from the current method presented in Section III. These figures, clearly show, that the calculated parameters are good candidates to properly model the dynamic behavior of the machine.

It should be noted, that the circuit order in the presented methodology is one less than that of the IEEE Std. 115-A, it turns out in different number of parameters, and so different values.

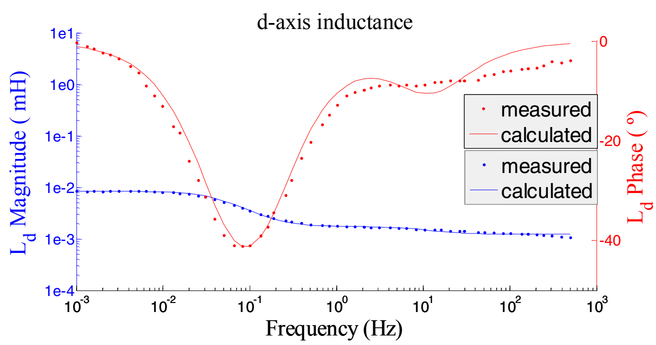

Fig. 12. Experimental and calculated d-axis operational inductance

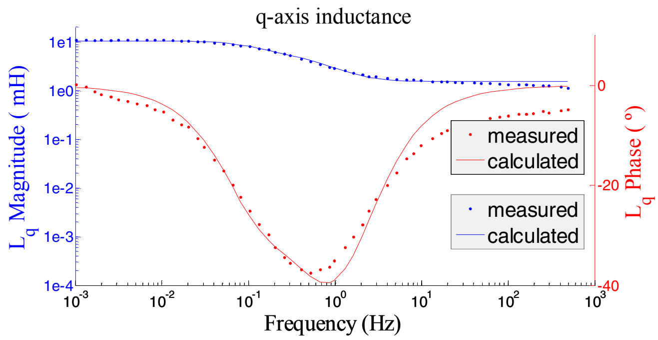

Fig. 2. Experimental and calculated q-axis operational inductance

The obtained parameters are:

R_a	0.0016[Ω]
R_{fd}	0.0021 [Ω]
R_{1d}	*0.0934* [Ω]
R_{1q}	*0.0126* [Ω]
R_{2q}	*0.0116* [Ω]
L_l	0.000795 [H]
L_{ad}	0.007155 [H]
L_{aq}	0.007155 [H]
L_{fd}	0.000985 [H]
L_{1d}	0.000617 [H]
L_{1q}	0.000522 [H]
L_{2q}	0.0109 [H]
T'_{d0}	3.89 [s]
T''_{d0}	0.0156 [s]
T'_{q0}	1.83 [s]
T''_{q0}	0.3251 [s]
T'_{d}	0.8018 [s]
T''_{d}	0.011 [s]
T'_{q}	0.999 [s]
T''_{q}	0.094 [s]

V. Conclusions

This works has presented a methodology for synchronous generators d-q equivalent circuit calculation parameters based on IEEE Std 115-A. The standard only shows the parameter fitting for a specific example where it is assumed some starting values for the undetermined elements. This yields to an iterative procedure in order to obtain the final parameter values. Besides there are some steps not detailed enough for educational purposes.

Whatever topology can be set. After from this topology the different transfer functions (d,q) are obtained using the symbolic toolbox, i.e. the cumbersome expression. On the other hand the performed measurements of the machine are fitted according of the chosen order. Therefore the transfer function coefficients are calculated, which have to match with the symbolic expression obtained once the circuit topology is fixed. The obtained values by the presented methodology are in good agreement with than that of reported experimentally. The novel and educational approach, is based on the fact that the order of the circuit can be whatever, even a customized circuit topology since the methodology does not rely on a set of a given formulation, but in a general and reproducible comprehensible approach, resulting fast and easy to implement.

VI. Acknowledgment

This work has been partially supported by the Generalitat de Catalunya under the project SGR 2017 SGR 967 and the European Commission through the Clean Sky program under the project 755332-AEMS-IdFit.

References

[1] A. Griffo, R. Wrobel, P. H. Mellor and J. M. Yon, "Design and Characterization of a Three-Phase Brushless Exciter for Aircraft Starter/Generator," in *IEEE Transactions on Industry Applications*, vol. 49, no. 5, pp. 2106-2115, Sept.-Oct. 2013

[2] R. Wamkeue, C. Jolette, A. B. M. Mabwe, and I. Kamwa, “Cross-identification of synchronous generator parameters from RTDR test time-domain analytical responses, ”*IEEE Trans. Energy Convers.*,vol. 26, no. 3, pp. 776–786, Sep. 2011.

[3] B. Zaker, G. B. Gharehpetian, M. Karrari and N. Moaddabi, "Simultaneous Parameter Identification of Synchronous Generator and Excitation System Using Online Measurements," in *IEEE Transactions on Smart Grid*, vol. 7, no. 3, pp. 1230-1238, May 2016

[4] F. Maurer, M. T. Xuan and J. J. Simond, "Two Full Parameter Identification Methods for Synchronous Machine Applying DC-Decay Tests for a Rotor in Arbitrary Position," in *IEEE Transactions on Industry Applications*, vol. 53, no. 4, pp. 3505-3518, July-Aug. 2017.

[5] H. Radjeai, A. Barakat, S. Tnani and G. Champenois, "Identification of synchronous machine by Standstill Frequency Response (SSFR) method - influence of the stator resistance -," *The XIX International Conference on Electrical Machines - ICEM 2010*, Rome, 2010, pp. 1-5.

[6] R. M. Saunders, "Synchronous-machine standstill frequency-response test data analysis," in *IEEE Transactions on Energy Conversion*, vol. 6, no. 3, pp. 564-571, Sep 1991.

[7] J. Bladh, M. Wallin, L. Saarinen and U. Lundin, "Standstill Frequency Response Test on a Synchronous Machine Extended With Damper Bar Measurements," in *IEEE Transactions on Energy Conversion*, vol. 31, no. 1, pp. 46-56, March 2016.

[8] E. C. Bortoni and J. A. Jardini, "A standstill frequency response method for large salient pole synchronous machines," in *IEEE Transactions on Energy Conversion*, vol. 19, no. 4, pp. 687-691, Dec. 2004.

[9] T. L. Vandoorn, F. M. De Belie, T. J. Vyncke, J. A. Melkebeek, and P. Lataire, “Generation of multisinusoidal test signals for the identification of synchronous-machine parameters by using a voltage-source inverter, ”*IEEE Trans. Ind. Electron.*, vol. 57, no. 1, pp. 430–439, Jan. 2010.

[10] S. Pillutla and A. Keyhani,“Neural network observers for on-line tracking of synchronous generator parameters, ”*IEEE Trans. Energy Conversion*, vol. 14, pp. 23–31, Mar. 1999

[11] Melgoza, R. Jesus, G. T. Heydt, and A. Keyhani,“An algebraic approach for identifying operating point dependent parameters of synchronous machine using orthogonal series expansions, ”*IEEE Trans. Energy Conversion*, vol. 16, pp. 92–98, Mar. 2001.

[12] H. B. Karayaka, A. Keyhani, G. T. Heydt, B. L. Agrawal and D. A. Selin, "Synchronous generator model identification and parameter estimation from operating data," in *IEEE Transactions on Energy Conversion*, vol. 18, no. 1, pp. 121-126, Mar 2003.

[13] B. Aubert, J. Régnier, S. Caux and D. Alejo, "Kalman-Filter-Based Indicator for Online Interturn Short Circuits Detection in Permanent-Magnet Synchronous Generators," in *IEEE Transactions on Industrial Electronics*, vol. 62, no. 3, pp. 1921-1930, March 2015.

[14] M. Karrari and O. P. Malik, "Identification of physical parameters of a synchronous Generator from online measurements," in *IEEE Transactions on Energy Conversion*, vol. 19, no. 2, pp. 407-415, June 2004.